Time Resolved Chirp Measurement Based on a Polarization-Maintaining Fiber

Mohamed Essghair Chaibi, Hoang Trung Nguyen, Christophe Gosset, Frédéric Grillot, and Didier Erasme

***Abstract*— In high-speed optical networks, quantifying both the intensity and the frequency behaviors of optical signals has become a crucial task to evaluate transmission performance. In this letter, we report on a new technique to characterize optical signals. It is based on low-cost components and its operating mode is easy to provide accurate and fast measurements. The proposed technique is experimentally validated with signals whose characteristics are known. It is also tested with different optical transmitters.**

***Index Terms*— Frequency chirp, interferometry, polarization-maintaining fiber.**

I. Introduction

IN OPTICAL networks, the easiest way to convey data from one point to another is modulating the intensity of light at the emitter and detecting it at the receiver with a simple photo-detector after propagation through an optical fiber. The intensity modulation (IM) of an optical field is always accompanied by the modulation of its phase (PM) and its frequency (FM), as the latter is the time derivative of the former. The way in which IM and FM modulations interact depends on several parameters such as the structure of the modulator and the modulation frequency. Although FM can not be detected at the receiver side, it has an important effect on the transmission performance. FM is usually seen as an unwanted effect: the spectral broadening that it generates interacts with the fiber chromatic dispersion and then causes inter-symbols interference (ISI) at the receiver. On the other hand, it was shown in [1] and [2] that the FM of a DFB laser can be exploited to generate single sideband (SSB) signals suitable for transmission through an intensity modulation/direct detection (IM/DD) dispersive channel. Thus, quantifying both FM and IM behaviors of an optical field becomes crucial. This is referred to as time resolved chirp (TRC) measurement.

Several techniques have been developed to characterize the TRC of optical transmitters. Among them, the frequency discriminator method has been extensively reported. It is based on an interferometer configuration used to convert the frequency deviation into an intensity variation detectable by a photo-detector. The implementations of this technique differ from each other on the used interferometer: Mach-Zehnder [3] and Fabry-Perot [4] interferometers are the most popular. While the first is bulky and requires a tunable delay line, the second is known for its nonlinear transmission.

In this letter, we present a new implementation of the frequency discriminator method. The used interferometer is a polarization-maintaining fiber (PMF) sandwiched between a polarizer and a phase shifting system. The latter consists of a half-wave plate, a quarter-wave plate and a polarizer, all of them can be independently rotated about the optical axis. The birefringence property of the PMF leads to considering its rapid and slow axes as the two arms of the interferometer when two linearly polarized beams propagate along them.

The rest of this letter is organized as follows: In section 2, we describe in details the proposed interferometer and the way to extract the IM and FM profiles of an optical field. In section 3, the experimental setup is described. In section 4, we present some results on different optical transmitters, including a DFB laser and a Dual-Electro-absorption Modulated Laser (D-EML). Finally, section 5 summarizes this letter.

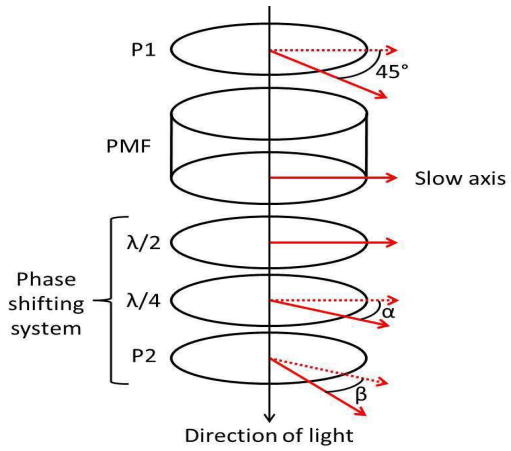

Fig. 1. Schematic diagram of the proposed interferometer. P: polarizer. $\lambda/2$ and $\lambda/4$ are the half-wave and the quarter-wave plates.

II. Operating Principle

A. The Interferometer

Let us consider an optical beam at the input of the proposed interferometer depicted in figure 1. It is generated by a continuous wave optical source. The optical field is expressed

Manuscript received February 24, 2015; revised May 4, 2015; accepted May 8, 2015. Date of publication May 11, 2015; date of current version June 24, 2015.

M. E. Chaibi, C. Gosset, F. Grillot, and D. Erasme are with the Department of Communications and Electronics, Institut Mines-Télécom, Télécom ParisTech, Paris 75634, France (e-mail: chaibi@telecom-paristech.fr; christophe.gosset@telecom-paristech.fr; frederic.grillot@telecom-paristech.fr; didier.erasme@telecom-paristech.fr).

H. T. Nguyen is with Apex Technologies, Marcoussis 91460, France (e-mail: hoang.trung.nguyen@apex-t.com).

Color versions of one or more of the figures in this letter are available online at http://ieeexplore.ieee.org.

Digital Object Identifier 10.1109/LPT.2015.2431853

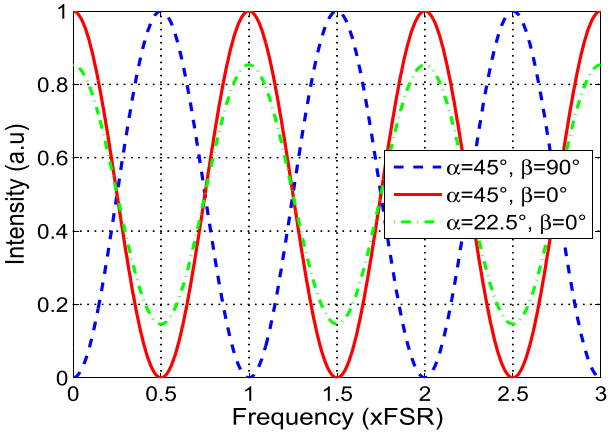

Fig. 2. Intensity transfer function of the interferometer for various couples (α, β).

in complex notation as:

$$E(t) = \sqrt{I_0} e^{j w_0 t} \tag{1}$$

Where I_0 is the average optical power and w_0 is the central angular frequency. The first polarizer of the interferometer is oriented at 45° with respect to the PMF birefringent axes, such an arrangement splits the input signal into two equal power, in-phase, independent modes whose linear polarization is aligned with the rapid and the slow axes of the PMF. This polarizer can be replaced by a half-wave plate, thus avoiding a 3 dB loss, provided availability of such a plate at the wavelength of operation. After propagation with different phase velocity along the axes of the PMF, the orthogonal components emerge with a differential phase shift that can be expressed as:

$$\Delta\theta = 2\pi \frac{\Delta n L}{\lambda} \tag{2}$$

Where Δn is the refractive index difference between the axes of the PMF whose length is L and λ is the emitted wavelength. The quantity $\Delta n L/c$, c being the light velocity in vacuum, is referred to as the free spectral range (FSR) of the interferometer. Consequently, the FSR can be easily adjusted by changing the fiber length. After passing through the half-wave and the quarter-wave plates, the rapid and slow components of the optical field interfere at the second polarizer. The intensity of light at the output of the interferometer may be expressed as:

$$I \propto [1 + \sin(2\alpha)\cos(2\beta)\cos(\Delta\theta) + \sin(2\beta)\sin(\Delta\theta)] \tag{3}$$

Here α is the quarter-wave plate orientation with respect to the half-wave plate and β denotes the orientation of the second polarizer with respect to the quarter-wave plate. For simplicity, the half-wave plate is kept aligned with the slow axis of the PMF. Equation 3 brings out two interesting points. Firstly, the extinction ratio of the interferometer depends solely on α with the best at $\alpha = 45°$. Secondly, β permits to easily shift the transfer function in the frequency domain. These two considerations are illustrated in figure 2 where equation 3 is plotted for various couples of (α,β). Contrary to similar implementations [5], the proposed interferometer is flexible in the way that its parameters including FSR, extinction ratio and peaks position are easily and independently adjustable. Therefore, it can be adapted to the wavelength of the input signal and the chirp that it may exhibit, and provides the required sensitivity to perform the frequency to intensity conversion. In the next subsection, we will explain how to extract the frequency deviation of a chirped signal using the described interferometer.

B. Frequency Chirp Measurement

Here we consider an optical signal modulated in both intensity and phase at the input of the interferometer. The optical field may be expressed as:

$$E(t) = \sqrt{I(t)} e^{j[w_0 t + \Phi(t)]} \tag{4}$$

Where $I(t)$ and $\Phi(t)$ are respectively the intensity and the phase modulation terms that we seek. Photo-detectors are only sensitive to the intensity of the field, i.e $I(t)$. To measure $\Phi(t)$, the proposed interferometer is used to convert the frequency deviation to an intensity variation thanks to its frequency-dependent transfer function. Keeping the notations of the previous subsection and setting $\alpha = 45°$ for a maximum of sensitivity, the optical power at the output of the interferometer is given by:

$$I_{out}(t) = [I(t) + I(t-\tau) + 2\sqrt{I(t)I(t-\tau)} \cos(\Delta\theta + \Delta\Phi(t) - 2\beta)] \tag{5}$$

Where τ, given by 1/FSR, denotes the time delay between the slow and fast axes and $\Delta\Phi(t) = \Phi(t) - \Phi(t-\tau)$. Varying β, we aim to extract $\Delta\Phi(t)$ and then the chirp by taking as many measurements as necessary. Three measurements are sufficient to retrieve $\Delta\Phi(t)$. The first one is $I(t)$ from which $I(t-\tau)$ is inferred. The two others, denoted by $I_{Q^+}(t)$ and $I_{Q^-}(t)$, are taken at $\Delta\theta - 2\beta = \pm 90°$. They correspond to the raising and falling quadrature points of the interferometer transfer function on which the frequency to intensity conversion is performed. The phase shift $\Delta\Phi(t)$ can be then expressed as a function of four intensity waveforms according to the following expression:

$$\Delta\Phi(t) = \arcsin\left(\frac{I_{Q^-}(t) - I_{Q^+}(t)}{I_{Q^-}(t) + I_{Q^+}(t)} \frac{I(t) + I(t-\tau)}{2\sqrt{I(t)I(t-\tau)}}\right) \tag{6}$$

The frequency chirp exhibited by the input signal defined as the time derivative of $\Phi(t)$ can be then expressed as [6]:

$$\Delta\nu(t) = F^{-1}\left\{\frac{F\{\Delta\Phi(t)\}}{2\pi \sum_{k=0}^{\infty} (-i\omega)^k \frac{\tau^{k+1}}{(k+1)!}}\right\} \tag{7}$$

F and F^{-1} denote respectively the Fourier transform and the inverse Fourier transform and ω is the frequency scale inferred from the time scale of one of the recorded measurements. In practice, the accuracy of measurements is strongly related to the choice of the FSR. Several considerations have to be taken into account when setting this value. Firstly, keeping the chirp amplitude variation within the linear region of the interferometer transfer function estimated at most at 12.5% of

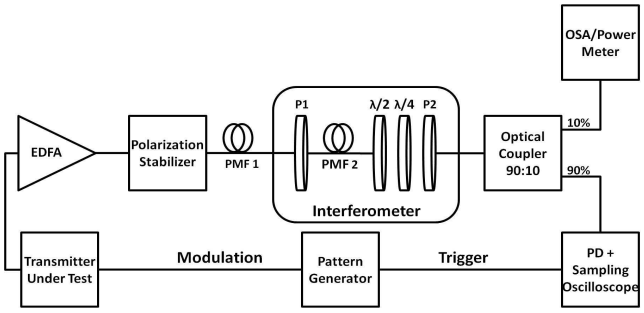

Fig. 3. Experimental setup.

the FSR [7] provides an easier linear analysis, optimizes the accuracy and reduces the consequence of a slight detuning for the quadrature point. Secondly, the time delay between the rapid and slow axes of the interferometer must remain well below the fastest modulation period.

III. Experimental Setup

The experimental setup used to measure the chirp of an input signal is shown in figure 3. A pattern generator modulates the optical transmitter and serves as a trigger for the oscilloscope. Sine and square signals at various frequencies are used for modulation. Transmitters tested with the proposed technique include a directly modulated DFB laser and a D-EML [8]. The latter is a DFB laser monolithically integrated with an electro-absorption modulator (EAM) with two independent accesses for modulation. For a matter of signal-to-noise ratio (SNR) and photo-diode (PD) sensitivity, optical signals are pre-amplified with an Erbium Doped Fiber Amplifier (EDFA). The FSR is visualized on an optical spectrum analyzer (OSA) using the amplified spontaneous emission (ASE) of the EDFA as a broadband input signal. Polarization is the basic idea behind the proposed technique, maintaining it stable at the input of the interferometer is important for the accuracy of measurements and the stability of the system. For this purpose, a polarization stabilizer is inserted in order to cope with rapid input state of polarization (SOP) fluctuations. Its output is a linearly polarized signal aligned with the slow axis of the first PMF whose axes are perfectly aligned with the second one. The same task may be performed by a Lefevre controller [9] for low cost implementations. The output of the interferometer is split with a 90:10 optical coupler. While 10% is sent to a power meter, 90% is detected by a 30 GHz photo-detector integrated on a sampling oscilloscope. The measurement process consists firstly in measuring $I(t)$ by setting the first polarizer at 0° with respect to PMF slow axes and $\alpha = \beta = 0°$. Then, the waveform $I(t-\tau)$ is inferred once τ is known. To measure $I_{Q^+}(t)$ and $I_{Q^-}(t)$, $\Delta\theta - 2\beta = \pm 90°$ are obtained without modulation by rotating clockwise and anticlockwise the second polarizer so as to get an optical power 3 dB below the maximum power. Modulation is then applied and measurements are taken. The four waveforms are off-line post-processed with Matlab to extract the intensity and the frequency profiles of the optical signal. If the measured chirp is not in agreement with the FSR restrictions mentioned in section 2, the PMF is changed to get the adequate value of FSR.

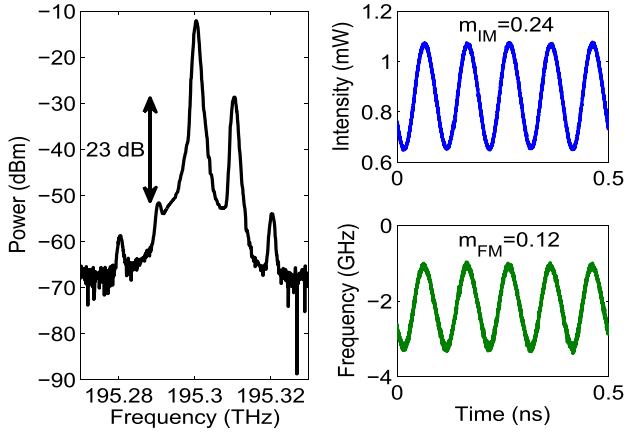

Fig. 4. Single sideband optical spectrum (black) with its intensity (blue) and frequency (green) profiles (FSR=35.6 GHz).

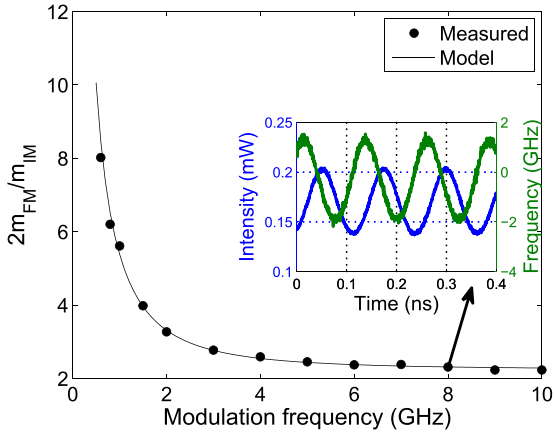

Fig. 5. Variation of the ratio between FM and IM indices with the modulation frequency (FSR=35.6 GHz). The inset illustrates the time responses for the intensity and for the optical frequency when the modulation frequency is 8 GHz.

IV. Results and Discussion

The proposed technique is tested with different optical transmitters with sinusoidal and pseudo-random modulating signals. To experimentally validate measurements provided by this technique, signals whose characteristics are known are characterized. For instance, SSB signals generated with a D-EML [8] are known to have an IM to FM index ratio equal to 2 and a phase shift between the two modulations of 0° or 180° depending on which sideband is eliminated. A 10 GHz SSB modulated signal is produced as it can be seen in figure 4. Its intensity and frequency profiles are measured and displayed without any kind of smoothing. They demonstrate that IM and FM are perfectly in-phase as expected and the indices ratio is exactly equal to 2. The proposed technique can also be used to extract the chirp parameters of optical transmitters. For a directly modulated DFB laser, we plot in figure 5 the variation of the ratio between FM and IM indices with the modulation frequency. The linewidth enhancement factor and the corner frequency [10], [11] respectively denoted by α and f_c can be easily extracted by fitting measurements with the theoretical model given by [12]:

$$\frac{2m_{FM}}{m_{IM}} = \alpha\sqrt{1+\left(\frac{f_c}{f_m}\right)^2} \tag{8}$$

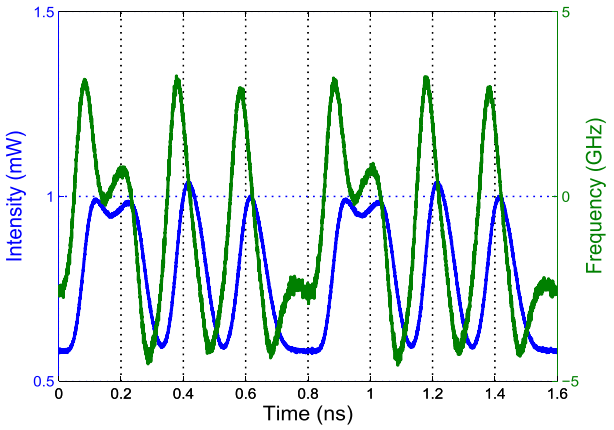

Fig. 6. Intensity and frequency profiles of a directly modulated DFB laser at 10 Gb/s (FSR=67.5 GHz).

Where m_{IM} is the IM index, m_{FM} is the FM index and f_m is the modulation frequency. α and f_c are respectively measured to 2.23 and 2.2 GHz. The same procedure allows to extract the chirp characteristics of several other transmitters such as EAM and semiconductor optical amplifier (SOA). The proposed technique is suitable for all forms of modulating signals and its flexibility allows full characterization of optical modulated signals. In figure 6, the sequence 01101010 carried at 10 Gb/s modulates the DFB laser. Once the intensity and the frequency profiles of the modulated signal are measured, transmission performance can be easily inferred as the channel response and the receiver noise are usually known.

V. Conclusion

A new setup to characterize the chirp of optical transmitters is presented. This setup is easy to be implemented as it is based on small-sized low-cost components. It can be used to extract the chirp parameters of optical transmitters and fully characterize optical modulated signals. In this context, a DFB laser and a D-EML were tested.

References

[1] M. E. Chaibi, D. Erasme, T. Anfray, C. Aupetit-Berthelemot, and C. Kazmierski, "Generation of SSB optical signals with dual-EML modulated with wideband OFDM," in *CLEO OSA Tech. Dig.*, Jun. 2014, pp. 1–2, paper SW1J.6.

[2] H. Kim, "EML-based optical single sideband transmitter," *IEEE Photon. Technol. Lett.*, vol. 20, no. 4, pp. 243–245, Feb. 15, 2008.

[3] J. P. King and I. Hardcastle, "Wideband chirp measurement technique for high bit rate sources," *Electron. Lett.*, vol. 30, no. 16, pp. 1336–1338, Aug. 1994.

[4] N. S. Bergano, "Wavelength discriminator method for measuring dynamic chirp in DFB lasers," *Electron. Lett.*, vol. 24, no. 20, pp. 1296–1297, Sep. 1988.

[5] A. Consoli, J. M. Tijero, and I. Esquivias, "Time resolved chirp measurements of gain switched semiconductor laser using a polarization based optical differentiator," *Opt. Exp.*, vol. 19, no. 11, pp. 10805–10812, 2011.

[6] C. Laverdiere, A. Fekecs, and M. Tetu, "A new method for measuring time-resolved frequency chirp of high bit rate sources," *IEEE Photon. Technol. Lett.*, vol. 15, no. 3, pp. 446–448, Mar. 2003.

[7] D. Derickson, *Fiber Optic Test and Measurement*. Englewood Cliffs, NJ, USA: Prentice-Hall, 1998, sec. 5.5.

[8] D. Erasme *et al.*, "The dual-electroabsorption modulated laser, a flexible solution for amplified and dispersion uncompensated networks over standard fiber," *J. Lightw. Technol.*, vol. 32, no. 21, pp. 4068–4078, Nov. 1, 2014.

[9] H. C. Lefevre, "Single-mode fibre fractional wave devices and polarisation controllers," *Electron. Lett.*, vol. 16, no. 20, pp. 778–780, Sep. 1980.

[10] R. Schimpe, J. E. Bowers, and T. L. Koch, "Characterisation of frequency response of 1.5 μm InGaAsP DFB laser diode and InGaAs PIN photodiode by heterodyne measurement technique," *Electron. Lett.*, vol. 22, no. 9, pp. 453–454, Apr. 1986.

[11] L. Olofsson and T. G. Brown, "Frequency dependence of the chirp factor in 1.55 μm distributed feedback semiconductor lasers," *IEEE Photon. Technol. Lett.*, vol. 4, no. 7, pp. 688–691, Jul. 1992.

[12] L. Anet Neto *et al.*, "Simple estimation of fiber dispersion and laser chirp parameters using the downhill simplex fitting algorithm," *J. Lightw. Technol.*, vol. 31, no. 2, pp. 334–342, Jan. 15, 2013.